JACS
JOURNAL OF THE AMERICAN CHEMICAL SOCIETY
Communication
pubs.acs.org/JACS

Single Turnover Reveals Oxygenated Intermediates in Toluene/*o*-Xylene Monooxygenase in the Presence of the Native Redox Partners

Alexandria Deliz Liang and Stephen J. Lippard*

Department of Chemistry, Massachusetts Institute of Technology, Cambridge, Massachusetts 02139, United States

Supporting Information

ABSTRACT: Toluene/*o*-xylene monooxygenase (ToMO) is a non-heme diiron protein that activates O_2 for subsequent arene oxidation. ToMO utilizes four protein components, a catalytic hydroxylase, a regulatory protein, a Rieske protein, and a reductase. O_2 activation and substrate hydroxylation in the presence of all four protein components is examined. These studies demonstrate the importance of native reductants by revealing reactivity unobserved when dithionite and mediators are used as the reductant. This reactivity is compared with that of other O_2-activating diiron enzymes.

Activation of O_2 by non-heme diiron enzymes generates reactive intermediates capable of hydrocarbon hydroxylation, epoxidation, desaturation, and radical formation.[1] Because structurally similar active sites catalyze diverse chemical transformations, the mechanisms by which these diiron enzymes control reactivity are of particular interest.

Toluene/*o*-xylene monooxygenase (ToMO) belongs to a family of diiron proteins termed bacterial multicomponent monooxygenases (BMMs) that activate O_2 to oxidize hydrocarbon substrates (Scheme 1).[2] ToMO catalyzes the hydroxylation of toluene to form *o*-, *m*-, and *p*-cresol and can also perform the catalytic, regiospecific hydroxylation of phenol to form catechol.[3] Four protein components are required to carry out efficient catalysis, a dimeric hydroxylase (ToMOH), a regulatory protein (ToMOD), a reductase (ToMOF), and a Rieske protein (ToMOC).[2a] Previous O_2-activation studies with ToMO utilized a simplified reaction comprising ToMOH, ToMOD, and sodium dithionite as a reductant with methyl viologen (2e-MV) as an electron-transfer mediator.[4] Reduction of ToMOH by ToMOC is important for efficient arene hydroxylation, however.[2a,5] Here we sought to determine how single turnover and O_2 activation by the native system, $ToMO_{red}$ (ToMOH, ToMOD, ToMOC, ToMOF, and NADH), differs from that observed using 2e-MV to reduce ToMOH. The latter produces a single colorless intermediate, $ToMOH_{peroxo}$.[4]

Scheme 1. General Mechanism for Hydroxylation by BMMs

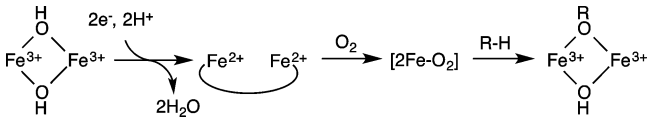

Under single-turnover conditions with limiting [NADH], the rate of phenol hydroxylation to form catechol by $ToMO_{red}$ and O_2 depends on the ratio of ToMOC to diiron sites of ToMOH, hereafter denoted as ToMOC:diiron (Figure 1). Using 0.01 ToMOC:diiron, 36(3)% of the diiron sites form catechol by 2 s with a rate constant of 8(1) s^{-1}. A slow increase in product formation ensues, and at 10 min, 84(4)% of the diiron sites produce catechol (Figure S1 in the Supporting Information). In contrast, using 1 ToMOC:diiron, 70(4)% of the diiron sites produce catechol by 2 s. These results suggest that inclusion of stoichiometric ToMOC promotes product formation by increasing the amount generated rapidly. The rate constant of each phase is not significantly affected by the ToMOC concentration, demonstrating that ToMOC does not directly participate in arene hydroxylation.

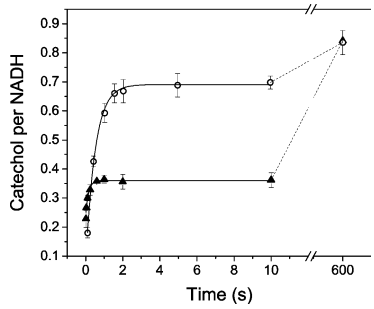

Figure 1. Hydroxylation of phenol to catechol at 4 °C during single turnover by ToMO. The concentrations of the components are as follows: 50 μM ToMOH (100 μM diiron sites), 100 μM ToMOD, 1 μM (▲) or 100 μM (○) ToMOC, 0.05 μM ToMOF, 90 μM NADH, 2 mM phenol, and approximately 625 μM O_2 (the O_2-saturated buffer contained ~1.25 mM O_2 at 5 °C; one-to-one mixing yielded 625 μM O_2).

Although some diiron proteins require substrate to bind prior to reduction,[6] preincubation of toluene monooxygenases with reductants provided the reduced hydroxylase.[4,7] In the single-turnover experiments reported here, product quantification requires rapid protein precipitation, which releases product bound at the active site. Thus, ToMOC must influence steps(s) between reduction of the diiron site and product release. These

Received: July 7, 2015
Published: August 12, 2015

DOI: 10.1021/jacs.5b07055
J. Am. Chem. Soc. 2015, 137, 10520−10523

steps could include O_2 activation, aromatic substrate binding, substrate hydroxylation, and any conformational changes necessary for the execution of each step.

In the presence of 0.01 ToMOC:diiron, O_2 activation by $ToMO_{red}$ generates absorption changes at 420 and 675 nm (Figure 2) that are not observed when 2e-MV is used as the

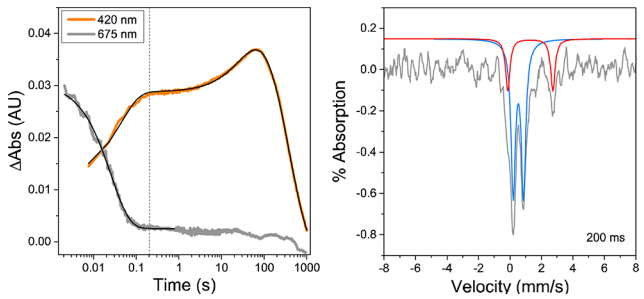

Figure 2. Analysis of O_2 activation upon mixing of dioxygen with $ToMO_{red}$ at 5 °C. (left) Time-resolved stopped-flow UV−vis spectroscopy of the reaction between $ToMO_{red}$ containing 0.01 ToMOC:diiron. The absorption changes at 420 and 675 nm are shown in orange and gray, respectively. Fits to the absorption traces are shown in black. (right) Mössbauer spectroscopy of the ToMOH diiron site at 0.2 s isolated by rapid freeze-quenching of a reaction containing 0.1 ToMOC:diiron. The data were recorded at 80 °C. The Mössbauer signal is shown in gray, and the simulated fits are shown in light blue for the Fe^{3+} intermediate (δ = 0.54 mm/s and ΔE_Q = 0.67 mm/s, 80%) and in red for unreacted Fe^{2+} starting material (δ = 1.31 mm/s and ΔE_Q = 2.88 mm/s, 20%).

reductant.[4] These absorption changes are absent when either hydroxylase or O_2 is omitted (Figure S2), indicating that the features result from reaction of O_2 with the hydroxylase. Because ToMOC contains a redox-dependent chromophore, higher ToMOC:diiron ratios were not suitable for monitoring O_2 activation by the diiron center.[8]

When the concentration of O_2 was varied between 375 and 625 μM, the observed kinetics was unchanged (Figure S3 and Table S1), indicating that the interaction of ToMOH with O_2 must be faster than the first observable step, as found for related diiron enzymes.[9] The simplest interpretation of these data invokes the formation of four species: 675A, $t_{max} \leq 2$ ms, k_{decay} = 40(5) s^{-1}; 420A, t_{max} = 200 ms, $k_{formation}$ = 23(1) s^{-1}; 420B, $t_{max} \sim 70$ s, $k_{formation}$ = 0.023(2) s^{-1}; and H_{ox}, $t_{max} > 1000$ s, $k_{formation}$ = 0.0018(2) s^{-1}.

The maximum accumulation of 675A occurs before the mixing time of the instrument (2 ms), which limits the ability to fully characterize this species by rapid mixing techniques. Intermediates 420A and 420B were characterized by rapid freeze-quench (RFQ) Mössbauer spectroscopy.[10] RFQ Mössbauer reactions were conducted at 0.1 ToMOC:diiron and 1 ToMOC:diiron. The two sample conditions yielded similar Mössbauer parameters (Figure S4).

Species 420A has a broad absorption band at 420 nm (Figure S5) that accumulates with a rate constant similar to that observed for $ToMOH_{peroxo}$ (~26 s^{-1}), the colorless intermediate previously reported when 2e-MV was used to reduce ToMOH.[4] For a sample frozen after 0.2 s, approximately 80% of the iron sites are iron(III) with Mössbauer parameters δ = 0.54 mm/s and ΔE_Q = 0.67 mm/s (Figure 2). The isomer shift and quadruple splitting are identical to those reported for $ToMOH_{peroxo}$ (Figure S6).[4] The remaining 20% is iron(II) (δ = 1.31 mm/s and ΔE_Q = 2.88 mm/s), corresponding to unreacted reduced enzyme.[4,7] Species 420A is stable for >6 s. Because of its long lifetime, we initially questioned whether this species is a diiron−O_2 intermediate. Diiron−O_2 adducts with lifetimes from 3 s to 3 h have been reported, however.[11]

Given the significant difference in the absorption profiles of 420A and the colorless intermediate $ToMOH_{peroxo}$, these intermediates must differ. Altering the reaction pH did not quench the absorbance corresponding to 420A (Figure S7), showing that excess protons alone cannot induce formation of $ToMOH_{peroxo}$ rather than 420A. Thus, other changes must be required, such as a conformational change.

Generation of 420B and formation of H_{ox} occurs with rate constants significantly smaller than steady-state turnover (toluene hydroxylation, ~0.5 s^{-1}),[12] suggesting that these steps are not relevant to catalysis. Analysis of intermediate 420B is provided in the Supporting Information. The final species has negligible absorbance at 420 and 675 nm, consistent with the diiron(III) resting state, H_{ox}.

The absorption changes were also monitored in the presence of excess toluene (Figure 3). The decay of the first species,

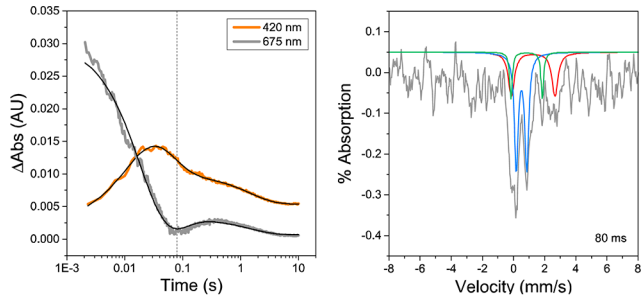

Figure 3. Analysis of O_2 activation upon mixing of O_2 and toluene with $ToMO_{red}$ at 5 °C. (left) Time-resolved stopped-flow UV−vis spectroscopy under the following conditions: 1 diiron, 1 ToMOD, 0.01 ToMOC, 0.0005 ToMOF, 0.9 NADH, 20 toluene, 6.25 O_2. The absorption changes at 420 and 675 nm are shown in orange and gray, respectively. Fits to the absorption traces are shown in black. (right) Analysis of intermediates at 0.2 s by rapid freeze−quench Mössbauer spectroscopy under the following conditions: 1 diiron, 1 ToMOD, 0.1 ToMOC, 0.0005 ToMOF, 0.9 NADH, 8 toluene, 1.25 O_2. The Mössbauer signal is shown gray, and the simulated species are shown in light blue (δ = 0.52 mm/s and ΔE_Q = 0.67 mm/s, 52%), green (δ = 0.845 mm/s and ΔE_Q = 2.01 mm/s, 27%), and red (δ = 1.26 mm/s and ΔE_Q = 2.79 mm/s, 20%).

675A, is unaffected by toluene, indicating that this species is not responsible for oxidizing aromatic substrates. In contrast, addition of toluene alters the absorption trace at 420 nm. The absorption trace at 420 nm is well-described by an A → B → C → D model with rate constants of 40(5) s^{-1}, 15(3) s^{-1}, and 0.61(4) s^{-1}. On the basis of the wavelength of maximum absorbance, rate of formation, and Mössbauer parameters, we assign the first species as intermediate 420A. The decay of 420A occurs rapidly in the presence of substrate (15 s^{-1}), consistent with 420A being responsible for substrate oxidation. Instead of forming H_{ox} directly, 420A decays to generate a species with $t_{max} \sim 0.5$ s (420-Ar), corresponding to toluene oxidation. The diiron(III) species 420-Ar is not observed in the absence of substrate and absorbs at both 420 and 675 nm. The rate constant for formation of 420-Ar is similar to that observed for hydroxylation of phenol in our single-turnover experiments above. Binding of phenolic derivatives to the diiron active site increases the absorbance at 420 and 675 nm (Figure S8). On

DOI: 10.1021/jacs.5b07055
J. Am. Chem. Soc. 2015, 137, 10520−10523

the basis of these observations, we assign 420-Ar as a cresol−diiron adduct resulting from hydroxylation of toluene.

In the final phase, 420-Ar decays with a rate constant of 0.61 s^{-1}, and the absorbance at 420 and 675 nm decreases. These changes are consistent with product release from the active site. The rate constant associated with this step is much smaller than that observed in our single-turnover experiments but is similar to the rate constant for steady-state turnover.[12] Thus, release of product may be rate-limiting for steady-state turnover, as previously proposed for the analogous BMM toluene 4-monooxygenase (T4MO) on the basis of X-ray crystallographic data.[13] O_2 activation in the presence of phenol proved to be much more complex than that observed with toluene (Figure S9), probably because of the formation of both diiron−phenol and diiron−catechol adducts.

Three important conclusions are evident from this work: (i) ToMOC is critical for the formation of an active hydroxylating species; (ii) the previously undetected species, 420A, decays rapidly upon addition of toluene, consistent with arene oxidation; (iii) ToMOH is capable of greater than half-sites reactivity.

The difference in reactivity between the natural system and the 2e-MV simulation is surprising given that the BMM soluble methane monooxygenase (sMMO) undergoes efficient single turnover using 2e-MV as the reduction system (Figure S10).[14] The non-heme diiron protein stearoyl-acyl carrier protein desaturase (Δ9D) also forms an inactive peroxo species when the diiron reducing protein is replaced with sodium dithionite.[15] For both ToMO and Δ9D, the reductases clearly promote activity, but it is also possible that dithionite inhibits activity, resulting in low turnover when dithionite present in excess.[2a,15]

A recent X-ray structure of the hydroxylase and Rieske protein complex for T4MO hints at a possible mechanism for Rieske protein function. In the 2.05 Å structure of the complex, residue E104 adopts a different conformation than those previously reported for BMMs (Figure 4A).[16] The new position

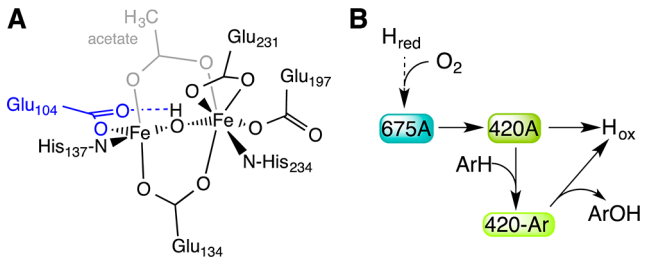

Figure 4. Influences of ToMOC on the activity of $ToMO_{red}$. On the basis of the Rieske−hydroxylase complex of T4MO, we propose that the unusual E104 conformation (A) may be responsible for the activity seen in the presence of ToMOC. A mechanistic scheme consistent with the activity of $ToMO_{red}$ is provided in (B).

of E104 alters the hydrogen bonding at the active site.[16] Computational analyses of peroxo intermediates formed at carboxylate-bridged diiron centers indicate that the transition near 420 nm corresponds to ligand-to-metal charge transfer from both the carboxylate and the peroxo ligands bound to the diiron site and that these transitions are sensitive to the carboxylate orientation.[17] Thus, the differing absorption features between the 2e-MV-reduced system and the $ToMO_{red}$ system may arise from conformational changes in E104. As to the structure, the newly discovered intermediate 420A may correspond to any one of many (hydro)peroxo−diiron conformations. Because 420A is long-lived and has Mössbauer properties similar to those observed and calculated for μ-1,2-peroxodiiron intermediates,[11d,16,17] we tentatively assign 420A as such a species.

Previous O_2-activation experiments reported half-sites reactivity with respect to the hydroxylase dimer.[4] The current work shows greater than 50% reactivity. This difference in activity may be a result of including ToMOC or of the ratio of O_2 to ToMOH used in our experiments. Here, 1.25 and 6.25 equiv of O_2 per diiron site are present in the Mössbauer and single-turnover studies, respectively. In previous Mössbauer and single-turnover studies,[4] we estimate that the ratios were 0.6 and 1.5, respectively, on the basis of the O_2 saturation methods (see the Supporting Information).

In summary, we have demonstrated the importance of the natural reduction system for efficient hydroxylation and O_2 activation by the multicomponent diiron protein ToMO. Using this knowledge, we were able to identify a previously unobserved species, 420A, during O_2 activation by the diiron protein ToMO. A proposed scheme that accounts for the observed O_2-activation kinetics is given in Figure 4B. Further insight into the effects of ToMOC at a molecular level would benefit from high-resolution structural data of the oxidized and reduced complexes between ToMOC and ToMOH.

■ ASSOCIATED CONTENT

Supporting Information

The Supporting Information is available free of charge on the ACS Publications website at DOI: 10.1021/jacs.5b07055.

Experimental details, evaluation of 420B, Figures S1−S10, and Tables S1−S3 (PDF)

■ AUTHOR INFORMATION

Corresponding Author

*lippard@mit.edu

Notes

The authors declare no competing financial interest.

■ ACKNOWLEDGMENTS

This work was supported by NIH Grant GM032134 from the National Institute of General Medical Sciences (NIGMS). A.D.L. was supported in part by the NIH NIGMS Biotechnology Training Program Grant T32 GM008334. The authors acknowledge Tsai-Te Lu and Woon Ju Song for helpful discussions.

■ REFERENCES

(1) Kurtz, D. M.; Boice, E.; Caranto, J. D.; Frederick, R. E.; Masitas, C. A.; Miner, K. D. In *Encyclopedia of Inorganic and Bioinorganic Chemistry*; John Wiley & Sons: Chichester, U.K., 2011.

(2) (a) Cafaro, V.; Scognamiglio, R.; Viggiani, A.; Izzo, V.; Passaro, I.; Notomista, E.; Dal Piaz, F.; Amoresano, A.; Casbarra, A.; Pucci, P.; Di Donato, A. *Eur. J. Biochem.* **2002**, *269*, 5689. (b) Leahy, J. G.; Batchelor, P. J.; Morcomb, S. M. *Fems Microbiol Rev.* **2003**, *27*, 449.

(3) Cafaro, V.; Notomista, E.; Capasso, P.; Di Donato, A. *Appl. Environ. Microb* **2005**, *71*, 4736.

(4) Murray, L. J.; Naik, S. G.; Ortillo, D. O.; García-Serres, R.; Lee, J. K.; Huynh, B. H.; Lippard, S. J. *J. Am. Chem. Soc.* **2007**, *129*, 14500.

(5) Tinberg, C. E.; Song, W. J.; Izzo, V.; Lippard, S. J. *Biochemistry* **2011**, *50*, 1788.

(6) Makris, T. M.; Chakrabarti, M.; Münck, E.; Lipscomb, J. D. *Proc. Natl. Acad. Sci. U. S. A.* **2010**, *107*, 15391.

DOI: 10.1021/jacs.5b07055
J. Am. Chem. Soc. 2015, 137, 10520−10523

(7) Pikus, J. D.; Studts, J. M.; Achim, C.; Kauffmann, K. E.; Münck, E.; Steffan, R. J.; McClay, K.; Fox, B. G. *Biochemistry* **1996**, *35*, 9106.
(8) Under these conditions, the maximum absorption changes for redox cycling of ToMOC and ToMOF are 3 mAU at 420 nm and 0.25 mAU at 675 nm.
(9) Stahl, S. S.; Francisco, W. A.; Merkx, M.; Klinman, J. P.; Lippard, S. J. *J. Biol. Chem.* **2001**, *276*, 4549.
(10) Only ToMOH was enriched with ^{57}Fe. The natural abundance of ^{57}Fe is 2%;[18] therefore, the spectra result exclusively from the iron atoms of ToMOH.
(11) (a) Vu, V. V.; Emerson, J. P.; Martinho, M.; Kim, Y. S.; Münck, E.; Park, M. H.; Que, L. *Proc. Natl. Acad. Sci. U. S. A.* **2009**, *106*, 14814. (b) Banerjee, R.; Meier, K. K.; Münck, E.; Lipscomb, J. D. *Biochemistry* **2013**, *52*, 4331. (c) Tinberg, C. E.; Lippard, S. J. *Biochemistry* **2009**, *48*, 12145. (d) Korboukh, V. K.; Li, N.; Barr, E. W.; Bollinger, J. M.; Krebs, C. *J. Am. Chem. Soc.* **2009**, *131*, 13608.
(12) Liang, A. D.; Lippard, S. J. *Biochemistry* **2014**, *53*, 7368.
(13) Bailey, L. J.; Acheson, J. F.; McCoy, J. G.; Elsen, N. L.; Phillips, G. N.; Fox, B. G. *Biochemistry* **2012**, *51*, 1101.
(14) (a) Liu, Y.; Nesheim, J. C.; Paulsen, K. E.; Stankovich, M. T.; Lipscomb, J. D. *Biochemistry* **1997**, *36*, 5223. (b) Valentine, A. M.; Stahl, S. S.; Lippard, S. J. *J. Am. Chem. Soc.* **1999**, *121*, 3876.
(15) (a) Broadwater, J. A.; Ai, J. Y.; Loehr, T. M.; Sanders-Loehr, J.; Fox, B. G. *Biochemistry* **1998**, *37*, 14664. (b) Sobrado, P.; Lyle, K. S.; Kaul, S. P.; Turco, M. M.; Arabshahi, I.; Marwah, A.; Fox, B. G. *Biochemistry* **2006**, *45*, 4848.
(16) Acheson, J. F.; Bailey, L. J.; Elsen, N. L.; Fox, B. G. *Nat. Commun.* **2014**, *5*, 5009.
(17) (a) Jensen, K. P.; Bell, C. B.; Clay, M. D.; Solomon, E. I. *J. Am. Chem. Soc.* **2009**, *131*, 12155. (b) Srnec, M.; Rokob, T. A.; Schwartz, J. K.; Kwak, Y.; Rulíšek, L.; Solomon, E. I. *Inorg. Chem.* **2012**, *51*, 2806.
(18) Drago, R. S. *Physical Methods for Chemists*, 2nd ed.; Saunders College Publishing: Fort Worth, TX, 1992.

DOI: 10.1021/jacs.5b07055
J. Am. Chem. Soc. 2015, 137, 10520−10523